



# The transformation of *nor-seco-cucurbit[10]uril* to cucurbit[5]uril and cucurbit[8]uril controlled by its own concentration

Shaojie Deng, Peihua Ma\*, Qinghong Bai, Xin Xiao\*

Key Laboratory of Macrocyclic and Supramolecular Chemistry of Guizhou Province, Department of Chemistry, Guizhou University, Guiyang 550025, China

## ARTICLE INFO

### Article history:

Received 12 January 2024

Revised 26 March 2024

Accepted 9 April 2024

Available online 9 April 2024

### Keywords:

*Nor-seco-cucurbit[10]uril*

Cracking

Transformation

Concentration control

Mechanism

## ABSTRACT

*Nor-seco-cucurbit[10]uril* (*ns*-CB[10]) is a kinetic product with unique structure. The single bridged methylene in its structure makes the molecular cavity of *ns*-CB[10] more deformable when compared to ordinary cucurbit[*n*]uril, reducing its structural stability. Repeated experiments showed that *ns*-CB[10] gradually cracks in an acidic solution and changes the specificity of cucurbit[5]uril (CB[5]) and cucurbit[8]uril (CB[8]) under more robust acidic solutions and when heated. A series of experiments were designed to study the transformation behavior of *ns*-CB[10]. It was found that the concentration of *ns*-CB[10] was correlated with the content distribution of CB[5] and CB[8]. This study explores the influencing factors and mechanisms of the transformation of *ns*-CB[10] to CB[5] and CB[8]. The results are of great significance for the application of *ns*-CB[10], understanding the formation mechanism of cucurbit[*n*]urils. Furthermore, it provides a new pathway for synthesizing new cucurbit[*n*]urils.

© 2024 Published by Elsevier B.V. on behalf of Chinese Chemical Society and Institute of Materia Medica, Chinese Academy of Medical Sciences.

Since Mock confirmed the structure of Behrend polymer in 1981 [1], cucurbit[*n*]uril (CB[*n*]) has attracted the attention of researchers in the realm of supramolecular chemistry over the past few decades. From the earliest discovered CB[6] to CB[5], CB[7], CB[8] [2], CB[10] [3], and larger twisted CB[*n*s] [4,5], the CB[*n*] family has also grown. The unique structure and excellent supramolecular chemical properties make the CB[*n*] family of great research interest in compound separation [6], drug delivery [7], catalysis [8], sensing [9–11], and new materials [12–14]. *Nor-seco-cucurbit[10]uril* (*ns*-CB[10]) prepared from glycoluril and paraformaldehyde in concentrated hydrochloric acid and mild temperature was reported by the Isaacs group in 2006 [15]. Although this is an earlier report, related research reports are quite rare [16–22].

The molecular cavity (peanut-like cavity) and existence of single bridged methylene in *ns*-CB[10] give it many unique properties when compared with the other members of the CB[*n*] family. Xiao *et al.* [23] found that it can efficiently and quickly separate pyridine from a mixture of toluene, benzene, and pyridine, and the cycle performance and separation degree are excellent. The other two connected cavities mean constructing multi-component supramolecular systems, which have tremendous applications in a variety of fields [24,25]. At the same time, the molecular cavity volume of *ns*-CB[10] is also affected by the chemical sub-

stances present in the environment. Huang and co-workers used molecules of different sizes to undergo assembly with *ns*-CB[10] and found that the cavity volume increased from 450 Å<sup>3</sup> to 740 Å<sup>3</sup> [15]. We obtained two crystal structures of *ns*-CB[10] from a formic acid and hydrochloric acid solution, respectively, as shown in Fig. 1; the solvent type had a significant effect on the crystal structure of *ns*-CB[10]. The existence of the single bridged methylene not only changes the rigidity of the glycoluril ring to a certain extent, but also exposes the N–H group with higher activity in the glycoluril unit in the dislocation link portion. The reaction of imidazolinone with *ns*-CB[10] was employed by Wittenberg and co-workers to obtain a cavity-separated derivative, showcasing the reactivity of the N–H group in the linking portion [26]. The shape variability and reactivity of the structure exist simultaneously, indicating the chemical instability of *ns*-CB[10].

Quite by chance, we crystallized and purified *ns*-CB[10] using 8 mol/L hydrochloric acid solution. After the solution was cooled and placed, a diamond-shaped crystal was obtained, and its structure confirmed to be CB[8] using single crystal X-ray diffraction. Subsequently, we used different conditions to perform multiple experiments for verification and the results are shown in Fig. 2. The *ns*-CB[10] was converted into CB[5] and CB[8] under strongly acidic and high temperature conditions. Subsequently, we re-evaluated the thermal and chemical stability of *ns*-CB[10] and studied its cracking and transformation mechanism in an acidic solution. In this process, a concentration-controlled product distribution phenomenon was observed. Based on the experimental results of <sup>1</sup>H

\* Corresponding authors.

E-mail addresses: [pghma@gzu.edu.cn](mailto:pghma@gzu.edu.cn) (P. Ma), [gyhxxiaoxin@163.com](mailto:gyhxxiaoxin@163.com) (X. Xiao).

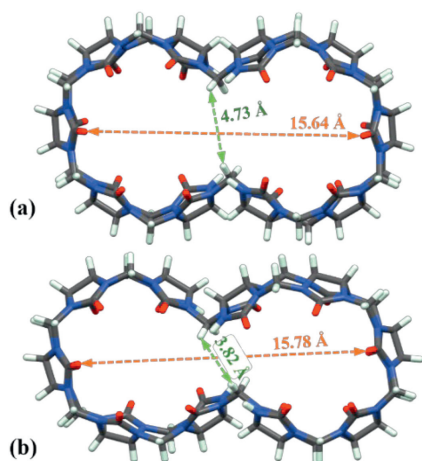


Fig. 1. Different crystal structures of *ns*-CB[10] in formic acid solution (a) and hydrochloric acid solution (b).

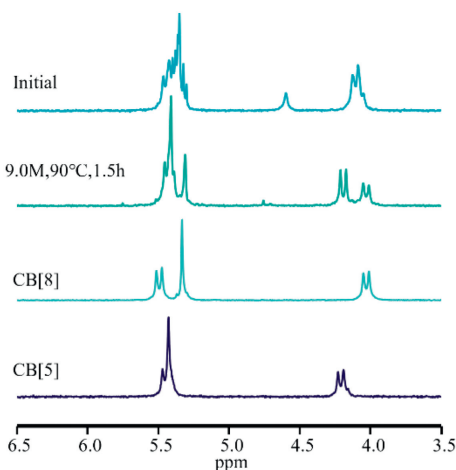


Fig. 2. The comparison of the <sup>1</sup>H NMR spectra obtained for *ns*-CB[10], CB[8], and CB[5] before and after heating. The solvent is 9.0 mol/L D<sub>2</sub>SO<sub>4</sub>, and the samples are measured at room temperature.

NMR, mass spectrometry, and quantum chemical calculation, a reasonable “fragment coupling” transformation mechanism was proposed, which provided a new idea for synthesizing new CB[*n*].

Thermogravimetric analysis performed under a nitrogen atmosphere (Fig. 3a) revealed that during the temperature ramping process, *ns*-CB[10] experienced a mass loss of 21.54% upon reaching 218.6 °C and it was not until the temperature rose to 318.1 °C that a further mass loss was observed. Its degradation temperature is slightly lower compared to other members of the family [27]. To determine if *ns*-CB[10] will decompose prior to attaining 318.1 °C, the sample will be subjected to continuous heating at 220 °C. <sup>1</sup>H NMR spectroscopy will be employed to monitor the sample both before and after the heating process. The spectra (Fig. 3b) revealed no discernible changes, indicating that the mass loss observed in the sample prior to 218.6 °C corresponds to the loss of crystalline water. This observation further suggested that *ns*-CB[10] exhibits thermal stability at temperatures < 318.1 °C.

Lucas and co-workers reported that *ns*-CB[10] is relatively easy to crack in an acidic solution [28]. However, the specific influencing factors were not investigated. We manipulated three distinct variables: Temperature, acidity, and time using D<sub>2</sub>SO<sub>4</sub>-D<sub>2</sub>O as the reaction medium to observe the cracking of *ns*-CB[10] via <sup>1</sup>H NMR spectroscopy. Due to the single bridged methylene characteristic peak of *ns*-CB[10], we can roughly obtain the content of *ns*-

CB[10] using the ratio of the integral area of the characteristic peak and low field shifted peak corresponding to the bridged methylene signal peak. Our results demonstrate that *ns*-CB[10] was prone to cracking in an acidic solution. Even when subjected to conditions of 4.5 mol/L D<sub>2</sub>SO<sub>4</sub> at 60 °C for 2 h, the content of *ns*-CB[10] decreased by 16.82%. Furthermore, the occurrence of cracking was observed even when the *ns*-CB[10] sample was left at room temperature for several days (refer to the <sup>1</sup>H NMR data corresponding to “3 d, 20 °C” in Fig. S34a in Supporting information). Figs. S20 and S21 (Supporting information) show that both the acidity and temperature can affect the cracking rate, but the effect of temperature was more significant. However, the stability of *ns*-CB[10] can be significantly enhanced if there are amine salts present within its cavity (Fig. S19 in Supporting information).

Although *ns*-CB[10] is quite prone to cracking, the temperature and acidic conditions required for its conversion to CB[5] and CB[8] are higher. Acidity has a more significant effect on the conversion behavior. At low acidity (4.5 mol/L D<sub>2</sub>SO<sub>4</sub>), CB[5] and CB[8] are hardly observed in terms of the low-field bridged methylene peak after 2 h of reaction, even at 80 °C (Fig. S5 in Supporting information). When the acidity is increased to 7.5 mol/L, the characteristic peaks of CB[5] and CB[8] can be observed at 80 °C after 30 min (Fig. S13 in Supporting information). The higher the acidity, the appearance of the characteristic signal peaks corresponding to CB[5] and CB[8] occurs at lower temperature in a shorter time. It is worth noting that even at 9.0 mol/L, the reaction was still not obvious at 60 °C, which may be the temperature barrier for the transformation.

In our verification and cracking experiments, different proportions of CB[5] and CB[8] appeared at the same temperature and acidity. Subsequently, we used various concentrations of the *ns*-CB[10] sample to react at 9.0 mol/L and 90 °C. It was found that the concentration of *ns*-CB[10] was the main factor controlling the distribution of CB[5] and CB[8], as shown in Table S2 (Supporting information). As the reaction proceeds, the distribution ratio of the product tends to be stable. After a reaction of 3 h, at a concentration of 0.0400 g/mL (19.1672 × 10<sup>-6</sup> mol/mL), CB[5] and CB[8] are present at comparable levels; below this threshold, CB[5] predominates, whereas above it, CB[8] marginally exceeds CB[5].

The formation-transformation mechanism of CB[*n*] has been reported [29–32], but we have shown the specific transformation of *ns*-CB[10] to CB[5] and CB[8] using many experiments gave results somewhat different from those reported in the literature. To further explore the reaction mechanism, the sample was gradually heated and <sup>1</sup>H NMR spectroscopy and mass spectrometry used to analyze the reaction solution at each reaction stage.

Some critical information was obtained and the results shown in Fig. S34a. CB[5] was first formed after the cracking of *ns*-CB[10] and was then gradually formed after some time. Subsequently, we decided to react *ns*-CB[10] with excess formaldehyde at two stages to observe its changes.

During the initial stage *ns*-CB[10] was mixed with excess paraformaldehyde and heated. It was found that the product mainly showed the characteristic peak corresponding to CB[5] (Fig. S34c in Supporting information). This indicates that *ns*-CB[10] first forms the glycoluril pentamer (or its hydroxymethyl derivative) after cracking.

Next, *ns*-CB[10] was heated at 9.0 mol/L for 2 h at 70 °C and the characteristic peak of CB[5] observed in the <sup>1</sup>H NMR spectrum. Subsequently, excessive paraformaldehyde was added and heated at 90 °C for 2 h. Fig. S34b (Supporting information) shows no obvious characteristic peaks corresponding to other CB[*n*]s were observed except CB[5] and the transition to CB[8] was inhibited. Excessive formaldehyde will inhibit the cracking of the glycoluril polymer [28], so this indicates that CB[8] was formed by the cracking of glycoluril polymers with a degree of polymerization of >8

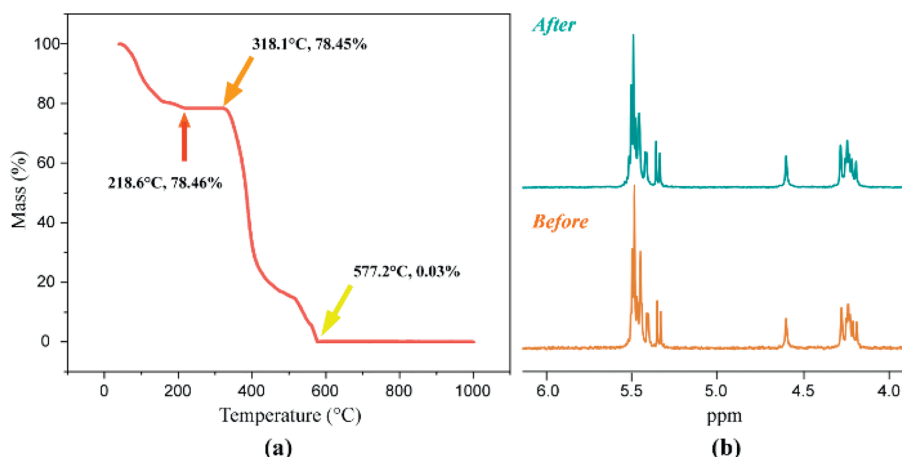
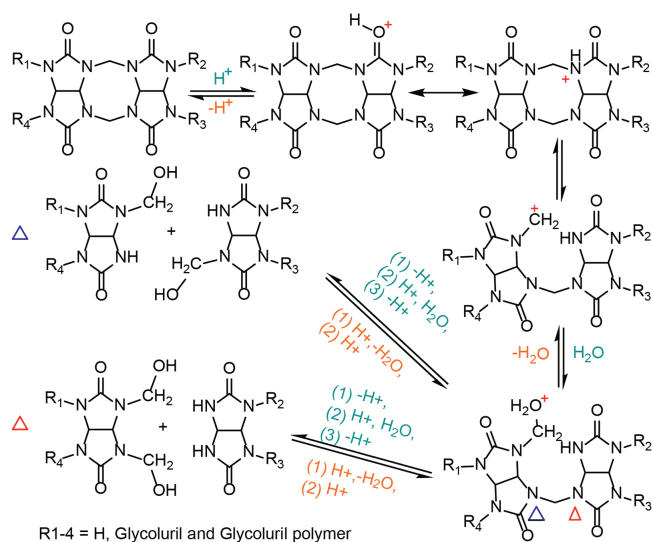


**Fig. 3.** (a) Thermogravimetric analysis of *ns*-CB[10] under a nitrogen atmosphere. (b)  $^1\text{H}$  NMR spectra obtained for the experimental samples before and after heating at 220 °C for 30 min under a nitrogen atmosphere; the NMR solvent was a 6.0 mol/L deuterated hydrochloric acid solution.

and was not formed by the “step-growth” [31] of glycoluril pentamers.

Identifying each peak in the mass spectrometry analysis of the whole stage was challenging due to unknown products and processes. However, we still obtained some helpful information from the relevant data (Figs. S35-S45 and Scheme S1 in Supporting information). The mass-to-charge ratio and relative abundance of ion peaks (above  $m/z$  590) in the analyzed samples showed consistent stability with no significant changes from the second to the ninth hour of the reaction. The data indicate that the fragments with a high mass-to-charge ratio originate from a single or consistent source.

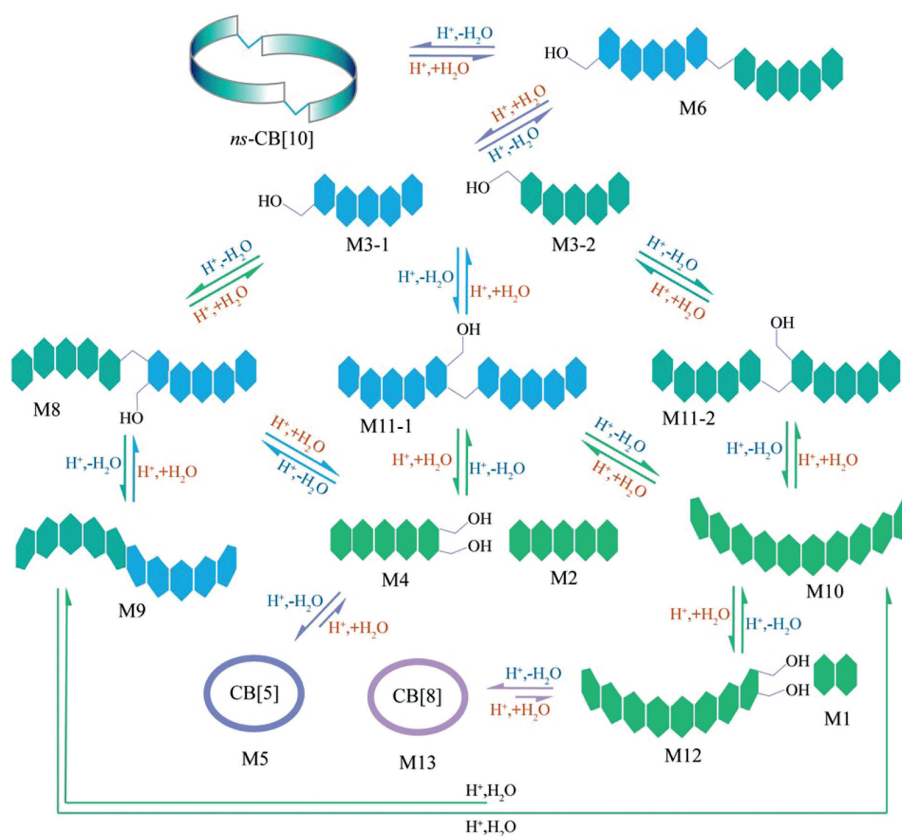
Based on the analysis of the  $^1\text{H}$  NMR spectra and mass spectrometry data, as well as referencing the relevant literature on the formation and transformation mechanisms of CB[ $n$ ] and its glycoluril polymer, as shown in Scheme 1, a proposed mechanism of “fragment coupling” was presented in Scheme 2. This mechanism suggests hydroxymethyl derivatives as intermediates for each reaction step. Furthermore, the hypothesis was supported using quantitative calculations. To facilitate our understanding, we simplified the molecular structure involved. For specific details regarding the corresponding structures, please refer to Section “Quantum chemical calculation” (Figs. S46-S49) in Supporting information.



**Scheme 1.** Cracking and formation mechanism of CB[ $n$ ]s and glycoluril polymers.

In an acidic aqueous solution, *ns*-CB[10] will first disconnect a single bridged methylene to form M6 (the acyclic glycoluril decamer reported by Huang co-workers [33], which can confirm the existence of M6). Subsequently, M6 undergoes cracking to form enantiomeric pairs M3-1 and M3-2. During the initial reaction stage, lower concentrations of the substances tend to favor the conversion of M3 to M8. M8 has two behaviors:  $\text{M8} \rightarrow \text{M9}$  and  $\text{M8} \rightarrow \text{M4} + \text{M2}$ ; the quantum chemical computations reveal that the energy difference ( $\Delta E$ ) between these two reactions was almost negligible, suggesting that the reactions are likely taking place under the control of Le Chatelier's principle. The propensity for the transformation from M4 to M5 was significantly pronounced. The “S” configuration glycoluril decamer (M9) needs to undergo configuration conversion to become M10 with a smaller energy “C” configuration ( $\Delta E = 7.5194$  kcal/mol). Subsequently, M10 undergoes fragmentation, resulting in the formation of M12, followed by dehydration to yield M13 (CB[8]). This explains why CB[5] was consistently observed first in our various experiments before the observation of CB[8]. As the reaction progressed, the concentrations of enantiomeric isomers M3-1 and M3-2 gradually increase, leading to the enhanced likelihood of molecular collisions and the subsequent formation of enantiomeric isomers M11-1 and M11-2. Their behavior was similar to M8, forming the glycoluril decamer or cracking to form M2 and M4. However, due to the energy differences within the reaction system and the control of Le Chatelier's principle, the reaction predominantly progresses toward forming M10. This is also the primary reason for the gradual increase in the content of CB[8] during the reaction.

In summary, we have systematically studied the stability of *ns*-CB[10] in a strongly acidic aqueous solution. This structurally peculiar CB[ $n$ ] has different instability from other family members. Although well-known as a kinetic product of CB[ $n$ ] synthesis, its decomposition in strong acid at room temperature is considered a surprising phenomenon. At higher temperature, its cracking rate is accelerated, and it will be further transformed into CB[ $n$ ] with a lower degree of polymerization after cracking. Although the ring contraction phenomenon has been proposed early on, it is remarkable that the transformation of *ns*-CB[10] exclusively leads to the formation of CB[5] and CB[8] with the ratio of CB[5] to CB[8] being solely dependent on the concentration of *ns*-CB[10]. However, the thermodynamically more stable CB[6] and CB[7] are conspicuously absent. This means that the transformation of CB[10] has some unique mechanisms. Based on our experimental results of each stage, we supplemented the “fragment coupling” mechanism to explain the specific transformation of *ns*-CB[10] to CB[5] and



**Scheme 2.** The “fragment coupling” mechanism of *ns*-CB[10] into CB[5] and CB[8]. Each hexagon in the figure represents a glycoside urea unit and the bridged methylene of the linked glycoside urea was omitted. Different colors were used to distinguish the different reaction pathways. To make the scheme look less cluttered, the chemical reaction symbol of the “M11-2→M2+M4” path was omitted.

CB[8], and verified its rationality using quantum chemical calculations. In this mechanism, two critical intermediates, M8 and the corresponding isomer M11, have been proposed. Their next behavior is affected by the energy of the reaction system and initial concentration of reactants, therefore we always observed the initial generation of CB[5] and different distribution ratios of CB[5] and CB[8] in our experiments.

The results of this study are of great significance for the subsequent application and preservation of *ns*-CB[10]. At the same time, a special hypothesis for the formation of CB[*n*]s has been proposed: Hydroxymethylated glycoluril polymers undergo coupling, followed by cleavage and cyclization, to form the cucurbituril structure. This complements and improves some of the mechanisms proposed for CB[*n*] formation-transformation. It also provides a new idea for filling the synthesis of CB[9] in CB[*n*] family members and the synthesis of CB[*n*]s with a higher degree of polymerization.

#### Declaration of competing interest

The authors declare that they have no known competing financial interests or personal relationships that could have appeared to influence the work reported in this paper.

#### CRediT authorship contribution statement

**Shaojie Deng:** Data curation, Methodology, Project administration, Validation, Writing – original draft, Software, Visualization. **Peihua Ma:** Resources, Writing – review & editing. **Qinghong Bai:** Software, Visualization. **Xin Xiao:** Conceptualization, Formal analysis, Validation, Writing – review & editing.

#### Acknowledgment

We acknowledge the financial support of National Natural Science Foundation of China (No. 22161010).

#### Supplementary materials

Supplementary material associated with this article can be found, in the online version, at doi:10.1016/j.ccl.2024.109878.

#### References

- [1] W.A. Freeman, W.L. Mock, N.Y. Shih, *J. Am. Chem. Soc.* 103 (1981) 7367–7368.
- [2] J. Kim, I.S. Jung, S.Y. Kim, et al., *J. Am. Chem. Soc.* 122 (2000) 540–541.
- [3] S. Liu, P.Y. Zavalij, L. Isaacs, *J. Am. Chem. Soc.* 127 (2005) 16798–16799.
- [4] X.J. Cheng, L.L. Liang, K. Chen, et al., *Angew. Chem. Inter. Ed.* 52 (2013) 7252–7255.
- [5] Q. Li, S.C. Qiu, J. Zhang, et al., *Org. Lett.* 18 (2016) 4020–4023.
- [6] H. Wu, Y. Wang, L.O. Jones, et al., *Angew. Chem. Inter. Ed.* 60 (2021) 17587–17594.
- [7] L.P. Cao, G. Hettiarachchi, V. Briken, L. Isaacs, et al., *Angew. Chem. Inter. Ed.* 52 (2013) 12033–12037.
- [8] G. Yun, Z. Hassan, J. Lee, et al., *Angew. Chem. Inter. Ed.* 53 (2014) 6414–6418.
- [9] F. Biedermann, W.M. Nau, *Angew. Chem. Inter. Ed.* 53 (2014) 5694–5699.
- [10] S. Jiang, J. Yang, L. Ling, S. Wang, D. Ma, *Anal. Chem.* 94 (2022) 5634–5641.
- [11] C. Li, X. Li, Q. Wang, *Chin. Chem. Lett.* 33 (2022) 877–880.
- [12] F.K. Metze, I. Filipucci, H.A. Klok, *Angew. Chem. Inter. Ed.* 62 (2023) e202305930.
- [13] L. Mao, S. Li, X. Zhang, Z.T. Li, D. Ma, *Chin. Chem. Lett.* 35 (2024) 109326.
- [14] C. Li, J. Zhu, Q. Wang, *Dyes Pigments* 204 (2022) 110368.
- [15] W.H. Huang, S. Liu, P.Y. Zavalij, L. Isaacs, *J. Am. Chem. Soc.* 128 (2006) 14744–14745.
- [16] R. Nally, L. Isaacs, *Tetrahedron* 65 (2009) 7249–7258.
- [17] V. Lemaure, G. Carroy, F. Poussiguet, et al., *ChemPlusChem* 78 (2013) 959–969.
- [18] M.I. El-Barghouthi, H.M. Abdel-Halim, F.J. Haj-Ibrahim, K. Bodoor, K.I. Assaf, *J. Inclusion Phenomena Macroscopic Chem.* 82 (2015) 323–333.
- [19] G. Carroy, V. Lemaure, J. De Winter, et al., *Phys. Chem. Chem. Phys.* 18 (2016) 12557–12568.

- [20] K.M. Park, J.H. Roh, G. Sung, J. Murray, K. Kim, *Chem. Asian J.* 12 (2017) 1461–1464.
- [21] Y. Yang, X.L. Ni, J.F. Xu, X. Zhang, *Chem. Commun.* 55 (2019) 13836–13839.
- [22] X. Zhang, W. Wu, Z. Tao, X.L. Ni, *Beilstein J. Org. Chem.* 15 (2019) 1705–1711.
- [23] M. Liu, R. Cen, J.S. Li, et al., *Angew. Chem. Inter. Ed.* 61 (2022) e202207209.
- [24] R. Cen, M. Liu, X.N. Yang, et al., *Sens. Actuator. B: Chem.* 393 (2023) 134213.
- [25] R. Cen, M. Liu, H. Xiao, et al., *Sens. Actuator. B: Chem.* 378 (2023) 133126.
- [26] J.B. Wittenberg, M.G. Costales, P.Y. Zavalij, L. Isaacs, *Chem. Commun.* 47 (2011) 9420–9422.
- [27] D. Bardelang, K.A. Udachin, D.M. Leek, et al., *Cryst. Growth Des.* 11 (2011) 5598–5614.
- [28] D. Lucas, L. Isaacs, *Org. Lett.* 13 (2011) 4112–4115.
- [29] A. Day, A.P. Arnold, R.J. Blanch, B. Snushall, *J. Org. Chem.* 66 (2001) 8094–8100.
- [30] S. Liu, K. Kim, L. Isaacs, *J. Org. Chem.* 72 (2007) 6840–6847.
- [31] W.H. Huang, P.Y. Zavalij, L. Isaacs, *J. Am. Chem. Soc.* 130 (2008) 8446–8454.
- [32] D. Lucas, T. Minami, G. Iannuzzi, et al., *J. Am. Chem. Soc.* 133 (2011) 17966–17976.
- [33] W.H. Huang, P.Y. Zavalij, L. Isaacs, *Org. Lett.* 11 (2009) 3918–3921.